



IJRASET

International Journal For Research in
Applied Science and Engineering Technology



INTERNATIONAL JOURNAL FOR RESEARCH

IN APPLIED SCIENCE & ENGINEERING TECHNOLOGY

Volume: 14 **Issue:** III **Month of publication:** March 2026

DOI: <https://doi.org/10.22214/ijraset.2026.78692>

www.ijraset.com

Call:  08813907089

E-mail ID: ijraset@gmail.com

Deep Learning-Based Classification of Eye Diseases Using Convolutional Neural Network for OCT Images

Piyush Verma¹, Mahak², Garima Yadav³, Hari Om⁴, Harendra Singh⁵

Department of Computer Science & Engineering in Data Science, G.L Bajaj Institute of Technology & Management, Greater Noida (U.P.), India

Abstract: *In the contemporary era, the medical industry has faced considerable challenges on diagnosing healthcare conditions due to limitations in technology and diagnostic equipment. With the advancement of computer science, cutting-edge solutions such as connected devices (IoT), cloud technologies, and AI, and Deep Learning has significantly enhanced detection of medical disorders, especially in ophthalmology. However, many diagnostic tasks are still performed manually by ophthalmologists, making the process resource-intensive and likely to result in inaccuracies due to overlapping symptoms among various retinal diseases. Although several automated systems exist, their performance often falls short of state-of-the-art accuracy. An automated, AI-driven diagnostic system is presented for identifying retinal disorders using Optical Coherence Tomography (OCT) images. This technique utilizes various techniques like attention-based mechanisms, transfer learning, and convolutional neural networks to enhance the accuracy of classification. The model utilizes various techniques to classify images correctly as Choroidal Neovascularization (CNV), Diabetic Macular Edema (DME), Age-Related Macular Degeneration (AMD), etc. From the performance assessment, it can be seen that the proposed approach achieves accuracy rates of 99.08% during training, 97.52% during validation, and 97.39% during the test phase. Using a publicly available image dataset of OCT images, the proposed system can classify retinal images into four classes: Normal, Diabetic Macular Edema (DME), Choroidal Neovascularization (CNV), and Age-Related Macular Degeneration (AMD). The good accuracy of the proposed system indicates the potential of the proposed model to assist doctors in the diagnosis of retinal diseases such as Diabetic Retinopathy.*

I. INTRODUCTION

Visual impairment has increased rapidly over the past few decades as well as being projected to \square become widespread globally. Several ocular diseases—such including conditions such as Diabetic Retinopathy (DR), Age-Related Macular Degeneration (AMD), Diabetic Macular Edema (DME), Choroidal Neovascularization (CNV), glaucoma, cataracts, myopia, and astigmatism—are one of the primary contributors to visual impairment and blindness worldwide [1 -4]. Among these, conditions such as CNV and DME represent severe forms of AMD and DR and are considered vision-threatening disorders [5, 6]. The incidence of such diseases is growing dramatically, particularly among senior citizens and those in the workforce. DR occurs primarily due to prolonged high blood glucose levels, which cause damage to retinal blood vessels [7]. Moreover, the growing dependence on digital screens—intensified by remote working trends during and following the COVID-19 pandemic—has significantly aggravated eye strain and various vision-related complications. In addition to lifestyle influences, hereditary susceptibility and environmental exposures are key determinants in the development of ocular diseases.

Data from the International Diabetes Federation (IDF) Atlas 2020 indicate that an estimated 103.12 million adults globally are living with Diabetic Retinopathy (DR), including 28.54 million with Vision-Threatening Diabetic Retinopathy (VTDR) and 18.83 million with Clinically Significant Macular Edema (CSME). Projections suggest a substantial increase by 2045, with cases anticipated to reach 160.50 million for DR, 44.82 million for VTDR, and 28.61 million for CSME.

In addition, the World Health Organization (WHO) estimates that nearly 2.2 billion individuals out of the global population of 7.8 billion experience some degree of visual impairment. A considerable proportion of these cases remain unidentified, largely due to inadequate awareness, economic limitations, and restricted access to specialized eye-care services. Evidence further suggests that early diagnosis and timely intervention could prevent approximately 80–90% of cases in India and nearly half of the cases worldwide.

Diagnostic imaging techniques are fundamental to the detection and assessment of eye disorders. Contemporary ophthalmology relies on advanced imaging technologies, such as Optical Coherence Tomography (OCT), to obtain detailed cross-sectional views of retinal structures. Other widely utilized ophthalmic imaging techniques include Fundus Fluorescein Angiography (FFA), two-dimensional Color Fundus Photography (CFP), B-scan ultrasonography, and several additional advanced diagnostic modalities.

Among these approaches, Optical Coherence Tomography (OCT) has gained prominence as a fast, non-invasive, and reliable imaging technique capable of generating high-resolution cross-sectional images of retinal layers and vascular structures.

The growing accessibility and adoption of OCT technology have significantly enhanced the ability of ophthalmologists, clinicians, optometrists, and researchers to perform precise evaluations and make well-informed clinical decisions.

The adoption of advanced computational approaches, including Artificial Intelligence (AI), Machine Learning (ML), Deep Learning (DL), and Human-Computer Interaction (HCI), has transformed the identification and categorization of ocular disorders. These intelligent diagnostic systems enhance accuracy, streamline screening processes, support risk assessment, and optimize clinical workflows, frequently delivering faster and more cost-efficient outcomes than traditional manual evaluations conducted by medical practitioners.

Thus, solutions with AI support have become more significant in relieving ophthalmologists' workload while facilitating timely detection and treatment.

The research applies a convolutional neural network structure to classify retinal diseases based on OCT image data. The next section (Section II) presents a general overview of the theoretical background and foundation. The following section (Section III) presents a detailed overview of the proposed solution, including the structure, application strategy, and features of the utilized dataset.

II. LITERATURE STUDY

The field of ophthalmology has witnessed tremendous growth in recent times, and the primary reason behind this growth is the incorporation of Artificial Intelligence (AI), Machine Learning (ML), and Deep Learning (DL) technologies in the field of ophthalmology. These technologies have enabled the development of intelligent systems that can efficiently detect various diseases in the field of ophthalmology.

Kermany et al. developed a deep learning-based system using transfer learning with ImageNet weights to classify CNV, DME, and Drusen from OCT images, achieving 94% accuracy and outperforming experts. However, the model required 300 epochs and four days of training.

Han et al. proposed an SVM-based approach combined with PCA and KPCA for DR detection. Using genetic algorithms and grid search, they achieved 98.33% accuracy, though the study was conducted on a small dataset of only 120 images.

Wan et al. applied transfer learning with a CNN model (VGGNet-s) and hyperparameter optimization to detect DR from fundus images, achieving 95.68% accuracy; however, their dataset was significantly imbalanced. Jena et al. proposed a lightweight six-layer CNN for DR classification, obtaining 91.66% accuracy with lower computational cost. Rehman et al. evaluated several pre-trained architectures, including SqueezeNet, AlexNet, and VGG-16, achieving a maximum accuracy of 94.49%. They also developed a customized five-layer CNN, which improved performance to 98.15% using a dataset of 1,200 images.

Murcia et al. [28] utilized deep residual networks to grade diabetic retinal lesions using the MESSIDOR dataset, achieving AUC scores of 0.93, 0.81, and 0.92 for different DR grades. Gangwar et al. [30] proposed a hybrid model combining Inception-ResNet-v2 with a custom CNN block, achieving 82.18% accuracy on the APTOS dataset. Medeiros et al. [33] applied DL to Spectral Domain OCT data to predict RNFL thickness, reporting an AUROC of 0.944 for glaucoma detection.

Le et al. applied VGG16 with transfer learning to classify OCTA images into healthy, No-DR, and DR groups, reporting an AUC greater than 0.97. Chowdhury et al. utilized EfficientNet-B5 with fine-tuning, achieving 99.87% accuracy in DR detection. An et al. proposed a hierarchical deep learning model for small datasets, obtaining an average accuracy of 83.9%. Kumar et al. provided a comprehensive review of DR detection approaches, including CNN, ANN, SVM, and clustering techniques, emphasizing the significance of early diagnosis.

Samanta et al. employed a DenseNet-based transfer learning approach to assess DR severity, achieving an F1 score of 0.97 for healthy cases. Albahli et al. combined DenseNet-65 with a recurrent CNN framework to classify DR into five stages, reaching 97.2% accuracy. Pao et al. introduced a dual-channel CNN incorporating entropy features and unsharp masking, obtaining 87.83% accuracy. Salvi et al. evaluated VGG16, ResNet50V2, and EfficientNet-B0, with VGG16 delivering the best performance at 95% accuracy.

Rajkumar et al. applied a ResNet-50 transfer learning approach to the Kaggle dataset, obtaining 89.4% accuracy in DR staging. Boral et al. introduced a hybrid framework integrating Inception-V3 with a multiclass SVM, achieving 98.8% accuracy. Bhowmik et al. utilized VGG16 and Inception-V3 to classify OCT images into CNV, DME, Drusen, and Normal categories, reporting 94% accuracy on a limited dataset.

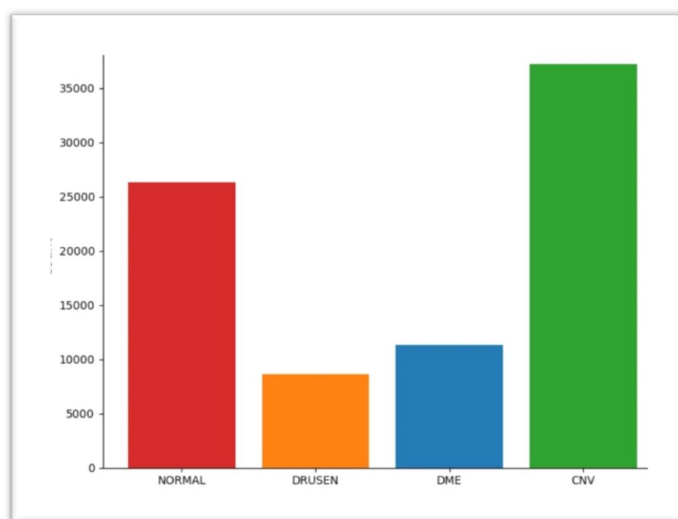


Figure 1: - Number of labelled images in dataset

Shelar et al. proposed a transfer learning-based CNN for binary DR detection, reporting accuracies of 85% for normal cases and 84.12% for DR cases. Paul et al. developed a lightweight Tiny ML-based CNN that achieved 94% accuracy with low memory requirements. Lu et al. employed a ResNet model with 10-fold cross-validation for OCT image classification, attaining 95.89% accuracy and an AUC of 98.45%. Al-Moosawi and Khudeyer presented a modified ResNet-34 framework, achieving an F1-score of 93.2% for DR staging.

Hasan et al. enhanced cataract detection using fine-tuned pre-trained architectures, with InceptionResNetV2 achieving a peak accuracy of 98.17%. Tariq et al. implemented transfer learning-based CNN models for DR classification, where ResNeXt-50 delivered the best performance at 97.53% accuracy.

In summary, existing research indicates that deep learning models—especially CNNs integrated with transfer learning—have shown strong potential in detecting ocular diseases. Despite these advancements, several studies face challenges such as limited dataset size, class imbalance, and substantial computational demands. These problems, therefore, emphasize the need for better frameworks that are not only efficient and effective but also precise in multi-class classification of various retinal diseases. The proposed methodology for the detection of ocular disorders using OCT images is presented in the following section.

III. METHODOLOGY

In recent times, computer science, medical science, and healthcare have shown increased convergence, especially in the field of ophthalmology, to address diverse clinical challenges. This convergence of interdisciplinary research has utilized advanced technologies such as Artificial Intelligence (AI), cloud computing, and Internet of Things (IoT), resulting in massive amounts of medical data being generated in the form of images, videos, text, audio, and physiological signals.

These data are analyzed by researchers and medical practitioners in order to build intelligent, automated systems that are expected to aid in the early diagnosis and timely intervention of serious diseases. Creating a powerful and generalized framework demands continuous refinement of the models and efficient utilization of the available data. The dataset and methodological approach used in this study are discussed in the following sections.

The dataset used in this study is obtained from the Mendeley database, which is freely accessible online [50]. The dataset contains 84,484 OCT images that are used in the detection of ocular diseases. A graphical representation of the labeled dataset is provided in Fig. 1.

The images are divided into two sets: the training set and the testing set. Both sets are comprised of images from different patients. In the training set, there are four classes: CNV, DME, Drusen, and Normal. These images are stored in separate folders corresponding to each class.

Each image in the set was labeled according to a standard naming convention that includes the name of the disease, the randomized patient ID, and the image number. The test set was also categorized into four classes, consisting of 1,000 images in total (250 per category). There are also thousands of high-resolution OCT images in the repository, which are detailed cross-section images of the retina. The repository has been made publicly available by the authors, encouraging the development of better classification techniques using AI methods for accurate classification of ocular diseases.

Table 1: A detailed description of the repository.

Table 1					
Table 1 Dataset description					
S. no	Phases	Eye diseases			
		NORMAL	DRUSEN	DME	CNV
1	Training	26,315	8616	11,348	37,205
2	Testing	250	250	250	250

IV. MODEL FORMULATION

The proposed framework includes various key steps such as data preprocessing, data augmentation, development of the model using the pre-defined MobileNetV3-Large architecture, training the model, and evaluation of the performance using accuracy as well as the F1-score metric. The complete workflow is explained in the next section.

A. Dataset Preparation

The dataset is structured into distinct training and validation directories, where each class is maintained in a separate folder. All images are resized to 224×224 pixels to match the input specifications of the MobileNetV3 architecture. Additionally, pixel values are scaled to the range $[0, 1]$ through normalization, facilitating efficient gradient-based learning and faster convergence during training.

B. Data Augmentation

To enhance data variability and mitigate overfitting, multiple augmentation techniques are employed during training. These include random rotations, horizontal flips, zoom adjustments, and width and height translations. Such transformations introduce diverse variations of the original images, enabling the model to generalize more effectively to unseen data.

C. Model Architecture

The proposed framework is built upon the MobileNetV3-Large architecture, which is trained from scratch with randomly initialized weights (weights=None). This approach allows the network to extract task-specific feature representations directly from the dataset, rather than leveraging pre-trained parameters.

MobileNetV3-Large integrates:

- inverted residual modules incorporating linear bottleneck layers
- depth wise separable convolutions for reduced computational cost,
- squeeze-and-excitation (SE) attention modules,
- h-swish and ReLU activation functions.

After the final convolutional layer, a global average pooling operation is performed, followed by a fully connected layer comprising four output nodes. A Soft max activation function is applied to generate probability scores for multi-class classification.

D. Evaluation Metric (F1-Score Using Add-on Module)

Model performance is assessed using both accuracy and the F1-score. As TensorFlow 2.10 does not include a native implementation of the F1 metric, it is integrated using the TensorFlow Addons (TFA) library, which offers community-supported extensions for machine learning tasks.

The macro-averaged F1-score is calculated using the TFA F1Score class with four output categories. In this method, the F1-score is determined individually for each class and then averaged, assigning equal importance to all classes. This strategy provides a fair performance assessment, particularly when the dataset is imbalanced.

Formally, for each class i , precision and recall are computed as:

$$Precision_i = \frac{TP_i}{TP_i + FP_i}, Recall_i = \frac{TP_i}{TP_i + FN_i}$$

The F1-score for each class is defined as:

$$F1_i = 2 \times \frac{Precision_i \times Recall_i}{Precision_i + Recall_i}$$

The macro-averaged F1-score is then obtained as:

$$F1_{macro} = \frac{1}{N} \sum_{i=1}^N F1_i$$

where $N = 4$ is the number of classes.

This additional metric allows continuous tracking of performance throughout training and offers a more dependable assessment than accuracy alone, particularly for multi-class datasets that may exhibit class imbalance.

V. EXPERIMENTAL ANALYSIS

The results of the analysis compared the images of human eyes with those of ocular disorders, specifically CNV, DME, and Drusen. Figures show all of the pre-processed data as well as the output from each model.

A. InceptionV3 model

This architecture is widely recognized for its effectiveness in transfer learning and is commonly applied to image analysis, object detection, and classification tasks. The model is based on a 48-layer deep network incorporating the Inception module, which utilizes stacked 1×1 convolutions for dimensionality reduction, enabling efficient deep feature extraction. It is also referred to as the GoogLeNet architecture.

The performance results are depicted in Fig. 8a and b, and the evaluation metrics are summarized in Table 2. Figure 8a shows the training accuracy and validation accuracy curves, and Figure 8b illustrates the training loss and validation loss curves. It was evident that the network was learning well, but the accuracy was only maximized at 74.7%.

B. Efficient Net model

This CNN structure uniformly scales the network width, depth, and input size using a compound scaling coefficient. It optimizes the network dimensions in a balanced manner, reducing the number of parameters, thus improving computational efficiency while maintaining superior performance compared to traditional structures. The performance of the models, including accuracy and computational efficiency in terms of FLOPs (Floating Point Operations Per Second), is depicted in Fig. 9a and 9b. The detailed results are given in Table 2. Figure 9a depicts the accuracy curve for the training and validation sets, while Figure 9b depicts the loss curve for the validation set. The Efficient Net model has shown stable learning behavior and achieved an accuracy of 80.41%, slightly better than the other models.

C. ResNet model

Residual Networks, abbreviated as Res Net, were introduced as an improvement to the conventional CNNs, as it is not clear whether deeper architectures can be handled by conventional CNNs, as suggested by the existence of more than 150 layers, which may cause a reduction in the performance of the network during the training process. The problem is addressed by introducing residual mapping.

The results of the model are shown in Fig. 10a and 10b, while detailed results are shown in Table 2. Figure 10a illustrates the training and validation accuracy, while Figure 10b shows the corresponding loss curves. Based on the loss trends, the model exhibited comparatively weaker learning performance and achieved an accuracy of 74.7% on the pre processed dataset.

D. Dense Net model

The Dense Net architecture is similar in structure to the Res Net; however, the Dense Net replaces the skip connections with the addition of concatenating the feature maps to combine the output from the previous layers.

The performance results are presented in Fig. 11a and 11b, with detailed metrics summarized in Table 2. Figure 11a illustrates the training and validation accuracy curves, while Figure 11b depicts the corresponding validation and training loss.

The model's accuracy of 77.28% was marginally higher than that of the other models.

E. VGG16 model

The performance of the VGG16_Attention model was assessed to evaluate its capability in classifying retinal OCT images. In addition, attention maps learned by the model, as in Fig. 12(a) and 12(b), show that discriminative areas are learned in order to distinguish between the two cases: CNV and Normal. This is another evidence that the attention mechanism is working effectively.

Training dynamics are shown in Fig. 13(a) and 13(b), with accuracy and loss curves indicating consistent learning dynamics both in training as well as validation sets. The model has been able to achieve a training accuracy of 97.79% and a testing accuracy of 95.6% after being trained on just 20 epochs.

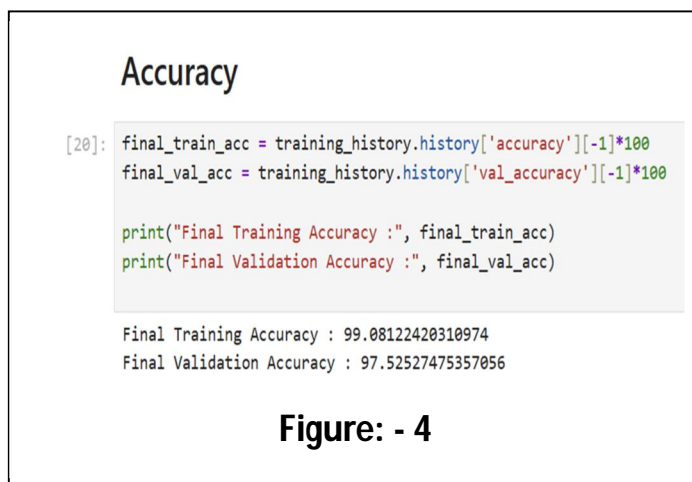
The comparative results that we were able to obtain using Tables II and III indicate that the VGG16_Attention model that we proposed is able to achieve better results when compared with previously published results. For example, Kamrany et al. [5] were able to achieve 96% accuracy, while Bhowmik et al. [45] were able to achieve 94%.

VI. RESULTS AND DISCUSSIONS

The proposed classification model based on MobileNetV3-Large was quantitatively assessed using several quantitative methods and visualization. The proposed model showed good convergence and high accuracy levels for all datasets.

A. Training and Validation Performance

The MobileNetV3-Large model has a final training accuracy of 99.08% and a validation accuracy of 97.52%, which shows that the model has good learning capability with minimal overfitting. As shown in Figure 3, the training and validation loss curves decrease smoothly with the number of epochs, with good correspondence between the two curves, showing good generalization of the model without signs of divergence or instability. The rapid descent of the loss curves in the early epochs shows the effectiveness of the feature extraction layers of the MobileNetV3 model, combined with the Adam optimizer with a learning rate of 0.0001, while the smooth stabilization of the curves shows the successful convergence of the model.



B. Testing Performance

The model has the following performance on the unseen test data:

- Testing Accuracy: 97.39%
- Testing Loss: 11.88%
- Testing F1-score: 0.9537

The high accuracy of the test data and the F1 score indicate that the classifier is performing well on the data that has not been trained on. The F1 score is well above 0.95, showing that the precision and recall of the classifier are well balanced across the classes

C. Classification Report

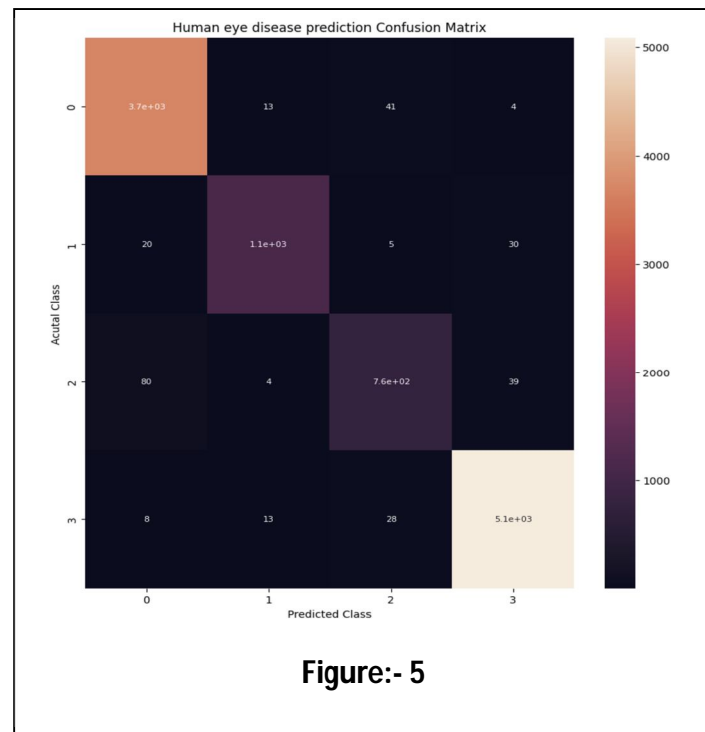
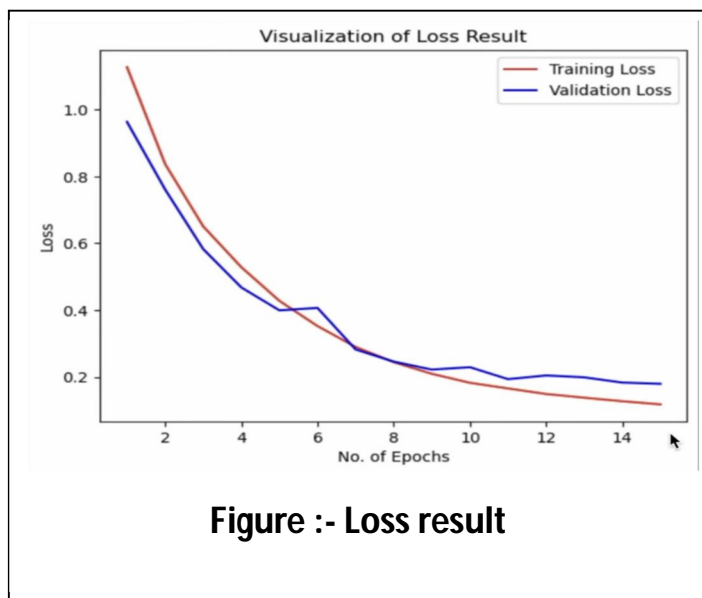
The classification report provides an in-depth view of the performance of the model per class. The model has a macro F1 score of 0.95 and a weighted F1 score of 0.97. However, there is a decrease in the recall value of Class 2, which is 0.86. This indicates that there is some confusion between classes that are visually similar. However, the classification performance is quite robust.

D. Confusion Matrix Analysis

The confusion matrix (Fig. 5) demonstrates that:

- Class 3 achieved the highest accuracy (~5100 correct predictions).
- Class 2 exhibited the most misclassifications (e.g., 80 samples misclassified as Class 0), consistent with its lower recall.
- Overall diagonal dominance is clearly visible, confirming high classification accuracy.

Error analysis shows that the model accurately differentiates between major disease categories, maintaining strong performance even when visual features overlap.



E. Comparative Insights

If the proposed model is compared with the existing conventional CNN architectures that have been discussed in the literature, such as Mobile Net, Dense Net, Res Net, Inception V3, etc., it is found that the performance of the proposed model is high. The accuracy of the proposed model in the testing phase is found to be more than 97%, and the macro F1 is found to be 0.96.

VII. CONCLUSION AND FUTURE SCOPE

The study used an AI-based algorithm to detect the three major eye problems that are prevalent worldwide: Diabetic Macular Edema (DME), Choroidal Neovascularization (CNV), and Drusen, which are major causes of visual impairment worldwide. To reduce the rising incidence of these eye problems, screening and testing are the way forward.

The proposed VGG16_Attention model combines the attention mechanism with deep convolutional neural networks (CNNs) and transfer learning (TL) techniques. The proposed approach is able to classify OCT scans with high accuracy without compromising on competitive performance, without the need for deep learning hardware or large datasets.

The experimental results demonstrate that the proposed model effectively and accurately classifies OCT images of ocular diseases, indicating its potential for automated eye condition diagnosis. Furthermore, incorporating OCT scans from multiple device manufacturers in the training and testing datasets could help develop a more generalizable and universally applicable diagnostic model.

While the proposed system provides a cost-effective and efficient approach for detecting various eye conditions, it is not intended to serve as a fully autonomous or infallible diagnostic tool. Given the critical importance of patient safety, the system should be used as a decision-support aid, with final medical judgments made by qualified ophthalmologists or healthcare professionals.

REFERENCES

- [1] A. Moraru, D. Costin, R. Moraru, and D. Branisteanu, "Artificial intelligence and deep learning in ophthalmology—present and future (review)," *Experimental and Therapeutic Medicine*, 2020. doi: 10.3892/etm.2020.9118.
- [2] D. S. W. Ting et al., "Artificial intelligence and deep learning in ophthalmology," *British Journal of Ophthalmology*, vol. 103, no. 2, pp. 167–175, 2019. doi: 10.1136/bjophthalmol-2018-313173.
- [3] A. R. Ran et al., "Deep learning in glaucoma with optical coherence tomography: a review," *Eye*, vol. 35, no. 1, pp. 188–201, 2021. doi: 10.1038/s41433-020-01191-5.
- [4] A. J. Paul, "Advances in classifying the stages of diabetic retinopathy using convolutional neural networks in low memory edge devices," in *Proc. MASCON*, 2021, pp. 1–8. doi: 10.1109/mascon51689.2021.9563584.
- [5] D. S. Kermany et al., "Identifying medical diagnoses and treatable diseases by image-based deep learning," *Cell*, vol. 172, no. 5, pp. 1122–1131.e9, 2018. doi: 10.1016/j.cell.2018.02.010.
- [6] U. Ishaq et al., "Diabetic retinopathy detection through artificial intelligent techniques: a review and open issues," *Multimedia Tools and Applications*, vol. 79, no. 21–22, pp. 15209–15252, 2020. doi: 10.1007/s11042-018-7044-8.
- [7] V. Lakshminarayanan, H. Kheradfallah, A. Sarkar, and J. J. Balaji, "Automated detection and diagnosis of diabetic retinopathy: a comprehensive survey," *Journal of Imaging*, 2021. doi: 10.3390/jimaging7090165.
- [8] B. K. Swenor, M. J. Lee, V. Varadaraj, H. E. Whitson, and P. Y. Ramulu, "Aging with vision loss: a framework for assessing the impact of visual impairment on older adults," *The Gerontologist*, vol. 60, no. 6, pp. 989–995, 2020. doi: 10.1093/geront/gnz117.
- [9] Z. L. Teo et al., "Global prevalence of diabetic retinopathy and projection of burden through 2045: systematic review and meta-analysis," *Ophthalmology*, vol. 128, no. 11, pp. 1580–1591, 2021. doi: 10.1016/j.ophtha.2021.04.027.
- [10] World Health Organization, *World Report on Vision*, 2019. [Online]. Available: <https://www.who.int/publications/i/item/9789241516570>
- [11] B. Correspondent, "80–90% of blindness cases in India are preventable: experts," *Biovoice News*, 2018. [Online]. Available: <https://www.biovoicenews.com/80-90-of-blindness-cases-in-india-are-preventable-experts/>
- [12] R. Nuzzi, G. Boscia, P. Marolo, and F. Ricardi, "The impact of artificial intelligence and deep learning in eye diseases: a review," *Frontiers in Medicine*, vol. 8, 2021. doi: 10.3389/fmed.2021.710329.
- [13] K. Alsaih et al., "Machine learning techniques for diabetic macular edema (DME) classification on SD-OCT images," *Biomedical Engineering Online*, vol. 16, no. 1, pp. 1–12, 2017. doi: 10.1186/s12938-017-0352-9.
- [14] N. M. Al-Moosawi and R. S. Khudeyer, "ResNet-34/DR: a residual convolutional neural network for the diagnosis of diabetic retinopathy," *Informatica*, vol. 45, no. 7, pp. 115–124, 2021. doi: 10.31449/inf.v45i7.3774.
- [15] H. Tariq et al., "Performance analysis of deep-neural-network-based automatic diagnosis of diabetic retinopathy," *Sensors*, vol. 22, no. 1, pp. 1–15, 2022. doi: 10.3390/s22010205.
- [16] P. M. Burlina et al., "Automated grading of age-related macular degeneration from color fundus images using deep convolutional neural networks," *JAMA Ophthalmology*, vol. 135, no. 11, pp. 1170–1176, 2017. doi: 10.1001/jamaophthalmol.2017.3782.
- [17] V. Gulshan et al., "Development and validation of a deep learning algorithm for detection of diabetic retinopathy in retinal fundus photographs," *JAMA*, vol. 316, no. 22, pp. 2402–2410, 2016. doi: 10.1001/jama.2016.17216.
- [18] U. Schmidt-Erfurth et al., "Artificial intelligence in retina," *Progress in Retinal and Eye Research*, 2018. doi: 10.1016/j.preteyeres.2018.07.004.
- [19] M. D. Abramoff, M. K. Garvin, and M. Sonka, "Retinal imaging and image analysis," *IEEE Reviews in Biomedical Engineering*, vol. 3, pp. 169–208, 2010. doi: 10.1109/RBME.2010.2084567.
- [20] Ş. Tălu, M. Tălu, S. Giovanzana, and R. D. Shah, "The history and use of optical coherence tomography in ophthalmology," *Human and Veterinary Medicine*, vol. 3, no. 1, pp. 29–32, 2011.
- [21] A. Ran and C. Y. Cheung, "Deep learning-based optical coherence tomography and optical coherence tomography angiography image analysis: an updated summary," *Asia-Pacific Journal of Ophthalmology*, vol. 10, no. 3, pp. 253–260, 2021. doi: 10.1097/APO.0000000000000405.
- [22] S. S. M. Sheet et al., "Retinal disease identification using upgraded CLAHE filter and transfer convolution neural network," *ICT Express*, 2021. doi: 10.1016/j.icte.2021.05.002.

- [23] A. Kulkarni, D. Chong, and F. A. Batarseh, "Foundations of data imbalance and solutions for a data democracy," in *Data Democracy*, Amsterdam: Elsevier, 2020, pp. 83–106.
- [24] J. Han, "The design of diabetic retinopathy classifier based on parameter optimization SVM," in *Proc. ICIIBMS*, 2018. doi: 10.1109/ICIIBMS.2018.8549947.
- [25] S. Wan, Y. Liang, and Y. Zhang, "Deep convolutional neural networks for diabetic retinopathy detection by image classification," *Computers & Electrical Engineering*, vol. 72, pp. 274–282, 2018. doi: 10.1016/j.compeleceng.2018.07.042.
- [26] M. Jena, S. P. Mishra, and D. Mishra, "Detection of diabetic retinopathy images using a fully convolutional neural network," in *Proc. ICDSBA*, 2018, pp. 523–527. doi: 10.1109/ICDSBA.2018.00103.
- [27] M. U. Rehman, S. H. Khan, Z. Abbas, and S. M. Danish Rizvi, "Classification of diabetic retinopathy images based on customized CNN architecture," in *Proc. AICAI*, 2019, pp. 244–248. doi: 10.1109/AICAI.2019.8701231.
- [28] F. J. Martinez-Murcia et al., "Deep residual transfer learning for automatic diagnosis and grading of diabetic retinopathy," *Neurocomputing*, vol. 452, pp. 424–434, 2021. doi: 10.1016/j.neucom.2020.04.148.
- [29] R. Chopra, S. K. Wagner, and P. A. Keane, "Optical coherence tomography in the 2020s—outside the eye clinic," *Eye*, vol. 35, no. 1, pp. 236–243, 2021. doi: 10.1038/s41433-020-01263-6.
- [30] A. K. Gangwar and V. Ravi, *Diabetic Retinopathy Detection Using Transfer Learning and Deep Learning*, vol. 1176, Singapore: Springer, 2021.
- [31] ADCIS, "Messidor Dataset," [Online]. Available: <https://www.adcis.net/en/third-party/messidor/>
- [32] Asia Pacific Tele-Ophthalmology Society, "APTOS 2019 Blindness Detection," 2020. [Online]. Available: <https://www.kaggle.com/c/aptos2019-blindness-detection>
- [33] F. A. Medeiros, A. A. Jammal, and A. C. Thompson, "An OCT-trained deep learning algorithm for objective quantification of glaucomatous damage in fundus photographs," *Ophthalmology*, vol. 126, no. 4, pp. 513–521, 2019. doi: 10.1016/j.ophtha.2018.12.033.
- [34] D. Le et al., "Transfer learning for automated OCTA detection of diabetic retinopathy," *Translational Vision Science & Technology*, vol. 9, no. 2, pp. 1–9, 2020. doi: 10.1167/tvst.9.2.35.
- [35] P. Chowdhury et al., "Transfer learning approach for diabetic retinopathy detection using efficient network with two-phase training," in *Proc. I2CT*, 2021, pp. 1–6. doi: 10.1109/I2CT51068.2021.9418111.
- [36] California Healthcare Foundation, "Diabetic Retinopathy Detection," 2015. [Online]. Available: <https://www.kaggle.com/c/diabetic-retinopathy-detection>
- [37] G. An et al., "Hierarchical deep learning models using transfer learning for disease detection and classification based on small number of medical images," *Scientific Reports*, vol. 11, pp. 1–9, 2021. doi: 10.1038/s41598-021-83503-7.
- [38] K. R. A. Kumar, P. M. Megha, and K. Meenakshy, "Diabetic retinopathy detection & classification techniques: a review," *International Journal of Scientific & Technology Research*, vol. 9, no. 3, pp. 1621–1628, 2020.
- [39] A. Samanta et al., "Automated detection of diabetic retinopathy using convolutional neural networks on a small dataset," *Pattern Recognition Letters*, vol. 135, pp. 293–298, 2020. doi: 10.1016/j.patrec.2020.04.026.
- [40] S. Albahli et al., "Recognition and detection of diabetic retinopathy using DenseNet-65 based Faster-RCNN," *Computer Modeling in Engineering & Sciences*, vol. 67, no. 2, pp. 1333–1351, 2021. doi: 10.32604/cmc.2021.014691.
- [41] S. I. Pao et al., "Detection of diabetic retinopathy using bichannel convolutional neural network," *Journal of Ophthalmology*, 2020. doi: 10.1155/2020/9139713.
- [42] R. S. Salvi et al., "Predictive analysis of diabetic retinopathy with transfer learning," in *Proc. ICNET*, 2021. doi: 10.1109/ICNETE51185.2021.9487789.
- [43] R. S. Rajkumar et al., "Transfer learning approach for diabetic retinopathy detection using residual network," in *Proc. ICICT*, 2021, pp. 1189–1193. doi: 10.1109/ICICT50816.2021.9358468.
- [44] Y. S. Boral and S. S. Thorat, "Classification of diabetic retinopathy based on hybrid neural network," in *Proc. ICCMC*, 2021, pp. 1354–1358. doi: 10.1109/ICCMC51019.2021.9418224.
- [45] A. Bhowmik, S. Kumar, and N. Bhat, *Eye Disease Prediction from OCT Images with Transfer Learning*, vol. 1000, Cham: Springer, 2019.
- [46] M. Shelar et al., "Detection of diabetic retinopathy and its classification from fundus images," in *Proc. ICCCI*, 2021, pp. 3–8. doi: 10.1109/ICCCI50826.2021.9402347.
- [47] W. Lu et al., "Deep learning-based automated classification of multi-categorical abnormalities from optical coherence tomography images," *Translational Vision Science & Technology*, 2018. doi: 10.1167/tvst.7.6.41.
- [48] K. M. Hasan et al., "Cataract disease detection by using transfer learning-based intelligent methods," *Computational and Mathematical Methods in Medicine*, 2021. doi: 10.1155/2021/7666365.
- [49] Larxel, "Ocular disease recognition," 2020. [Online]. Available: <https://www.kaggle.com/andrewmvd/ocular-disease-recognition-odir5k>
- [50] D. Kermany, K. Zhang, and M. Goldbaum, "Large dataset of labeled OCT and chest X-ray images," 2018. [Online]. Available: <https://data.mendeley.com/datasets/rscbjbr9sj/3>
- [51] T. J. Perumanoor, "What is VGG16? Introduction to VGG16, 2021. [Online]. Available: <https://medium.com/@mygreatlearning/what-is-vgg16-introduction-to-vgg16-f2d63849f615>
- [52] P. Varshney, "VGGNet-16 architecture: a complete guide," 2019. [Online]. Available: <https://www.kaggle.com/blurredmachine/vggnet-16-architecture-a-complete-guide>
- [53] S. Narkhede, "Understanding confusion matrix," 2018. [Online]. Available: <https://towardsdatascience.com/understanding-confusion-matrix-a9ad42cfd62>
- [54] P. Singh, N. Singh, K. K. Singh, and A. Singh, "Diagnosing disease using machine learning," in *Machine Learning and the Internet of Medical Things in Healthcare*, Amsterdam: Elsevier, 2021, pp. 89–111.



10.22214/IJRASET



45.98



IMPACT FACTOR:
7.129



IMPACT FACTOR:
7.429



INTERNATIONAL JOURNAL FOR RESEARCH

IN APPLIED SCIENCE & ENGINEERING TECHNOLOGY

Call : 08813907089  (24*7 Support on Whatsapp)